Quasi-elastic scattering and fusion with a modified Woods-Saxon potential

Ning Wang*
Department of Physics, Guangxi Normal University, Guilin 541004, People's Republic of China

Werner Scheid
Institut für Theoretische Physik der Universität, D-35392 Giessen, Germany

(Received 7 May 2008; revised manuscript received 10 June 2008; published 24 July 2008)

The elastic and large-angle quasi-elastic scattering reactions were studied with the same nucleus-nucleus potential proposed for describing fusion reactions. The elastic scattering angle distributions of some reactions are reasonably well reproduced by the proposed Woods-Saxon potential with fixed parameters at energies much higher than the Coulomb barrier. With an empirical barrier distribution based on the modified Woods-Saxon potential and taking into account the influence of nucleon transfer, the calculated quasi-elastic scattering cross sections of a series of reactions are in good agreement with the experimental data.

DOI: 10.1103/PhysRevC.78.014607 PACS number(s): 25.70.Bc, 25.70.Jj, 25.70.Hi

I. INTRODUCTION

Heavy-ion quasi-elastic scattering and fusion reactions at energies around the Coulomb barrier have been extensively studied in recent decades, because they provide an ideal opportunity to obtain the information of nuclear structure and nucleus-nucleus interaction and to explore the mechanism of heavy-ion reactions at near barrier energies that is of great importance for the synthesis of super-heavy nuclei [1–9]. Based on the quantum tunneling concept, it is thought that the quasi-elastic scattering (a sum of elastic scattering, inelastic scattering, and transfer channels) is a good counterpart of the fusion reaction in the sense that the former is related to the reflection probability of a potential barrier while the latter is related to the penetration probability [2]. In addition, it has been shown that the fusion barrier distribution generated by the coupling of the relative motion of the nuclei to internal degrees of freedom can be extracted from precisely measured fusion excitation functions [3,4]. The similarity of the barrier distribution can be extracted from large-angle quasi-elastic scattering excitation functions [5] that can be more easily measured than the fusion excitation functions [10]. Therefore, it is expected that both the fusion and quasi-elastic scattering cross sections of a heavy-ion reaction at energies around the Coulomb barrier can be unifiedly described by the same nucleus-nucleus potential. However, in recently published articles, Mukherjee *et al*. [11] found that the Woods-Saxon nuclear potential cannot simultaneously reproduce precise fusion and elastic scattering measurements of $^{12}C + ^{208}Pb$, and Muhammad and Hagino [12] found that the depth parameter of the Woods-Saxon potential for describing the fusion cross sections of $^{16}O + ^{144}Sm$ must be readjusted to reproduce the experimental quasi-elastic scattering cross sections of this reaction with the same coupled-channels framework. To solve this discrepancy, it is necessary to find a nucleus-nucleus potential for a unified description of the scattering and fusion data in heavy-ion reactions. In addition, to give satisfying predictions of quasi-elastic scattering cross sections for unmeasured reaction systems, it is required that a nucleus-nucleus potential be found to describe quasi-elastic scattering reactions systematically.

Studies of quasi-elastic scattering reactions and transfer processes, especially of the behavior of the transfer probabilities as functions of the distance of closest approach or the incident energies, have attracted a lot of attention. Some investigations show that the semiclassical method is suitable for describing the heavy-ion scattering at large reaction distance [13–16]. The transfer probability is expressed as an exponential function of the distance between the reaction partners $P_{tr} \propto \exp(-2\alpha R_c)$ [13] in the semiclassical approximation, where α is the transfer form factor and R_c is the distance of closest approach between two nuclei. The exponential dependence on R_c is a characteristic property of tunneling [15]. At energies below the barrier the experimental slopes are generally in good agreement with the predictions of the model for one-nucleon transfer. At higher energies, the measured slopes deviate from the calculated values, which is often referred to as "slope anomaly" in addition to other types of anomalies that are in connection with slopes obtained in two-particle transfer reactions [17]. Some experiments show an energy dependence of the slopes, and a clear trend of a decrease of slope parameters as a function of increasing energy was found in Refs. [16] and [17]. The transfer probabilities at below barrier energies have been extensively studied while a theoretical model for describing the slope parameters and the transfer probabilities at energies near and above the Coulomb barrier has not been well established yet. The study of the transfer probability in the latter energy region is still required. In addition, it is interesting to explore the relation between the transfer probabilities and the barrier distribution because the transfer probabilities generally peak in the vicinity of the barrier energies [10].

In Ref. [18] we proposed a modified Woods-Saxon potential model based on the Skyrme energy-density functional together with the extended Thomas-Fermi approach. This model was first proposed in Ref. [9] and a large number of fusion reactions have been described satisfactorily well with an

*wangning@gxnu.edu.cn

empirical barrier distribution that is based on the calculated entrance channel potential. In this work, we try to describe the heavy-ion elastic and quasi-elastic scattering with the same potential for describing the fusion reactions. The article is organized as follows: In Sec. II, the theoretical model for the description of the elastic and quasi-elastic scattering is introduced. In addition, some calculated results are compared with experimental data. The summary and discussion are given in Sec. III.

II. THEORETICAL MODEL FOR ELASTIC SCATTERING, QUASI-ELASTIC SCATTERING, AND FUSION

In this section, we first briefly introduce the modified Woods-Saxon potential and the elastic scattering is studied with the potential. In addition, the empirical barrier distribution is briefly introduced for describing fusion reactions. Then, the quasi-elastic scattering and the transfer probabilities are described with the empirical barrier distribution. Some calculated results are also presented in this section.

A. Modified Woods-Saxon potential and elastic scattering at above barrier energies

In Ref. [18] we proposed a Woods-Saxon potential model based on the Skyrme energy-density functional together with the extended Thomas-Fermi approach. The nucleus-nucleus interaction potential reads as

$$V(R) = V_N(R) + V_C(R). \tag{1}$$

Here, V_N and V_C are the nuclear and Coulomb interactions, respectively. We take $V_C(R) = e^2 Z_1 Z_2/R$, and the nuclear interaction V_N,

$$V_N(R) = \frac{V_0}{1+\exp[(R-R_0)/a]}, \tag{2}$$

with [19]

$$V_0 = u_0[1+\kappa(I_1+I_2)]\frac{A_1^{1/3}A_2^{1/3}}{A_1^{1/3}+A_2^{1/3}}, \tag{3}$$

and

$$R_0 = r_0\left(A_1^{1/3}+A_2^{1/3}\right)+c. \tag{4}$$

$I_1 = (N_1 - Z_1)/A_1$ and $I_2 = (N_2 - Z_2)/A_2$ in Eq. (3) are the isospin asymmetries of the projectile and target nuclei, respectively. In this potential, the depth of the potential V_0 depends on the reaction system and the isospin asymmetries. To distinguish it from the traditional Woods-Saxon potential (with three parameters) in which the depth of the potential is independent of the reaction system and the isospin asymmetries, we call the proposed potential (with five parameters) "modified" Woods-Saxon potential. The parameters of the modified Woods-Saxon (MWS) potential [18] are determined by the entrance channel potentials of 66,996 reactions obtained with the Skyrme energy-density approach and are listed in Table I.

TABLE I. Parameters of the modified Woods-Saxon potential.

r_0 (fm)	c (fm)	u_0 (MeV)	κ	a (fm)
1.27	−1.37	−44.16	−0.40	0.75

The proposed nucleus-nucleus potential is based on the frozen density approximation. The time-dependent Hartree-Forck (TDHF) calculations show that the nucleus-nucleus

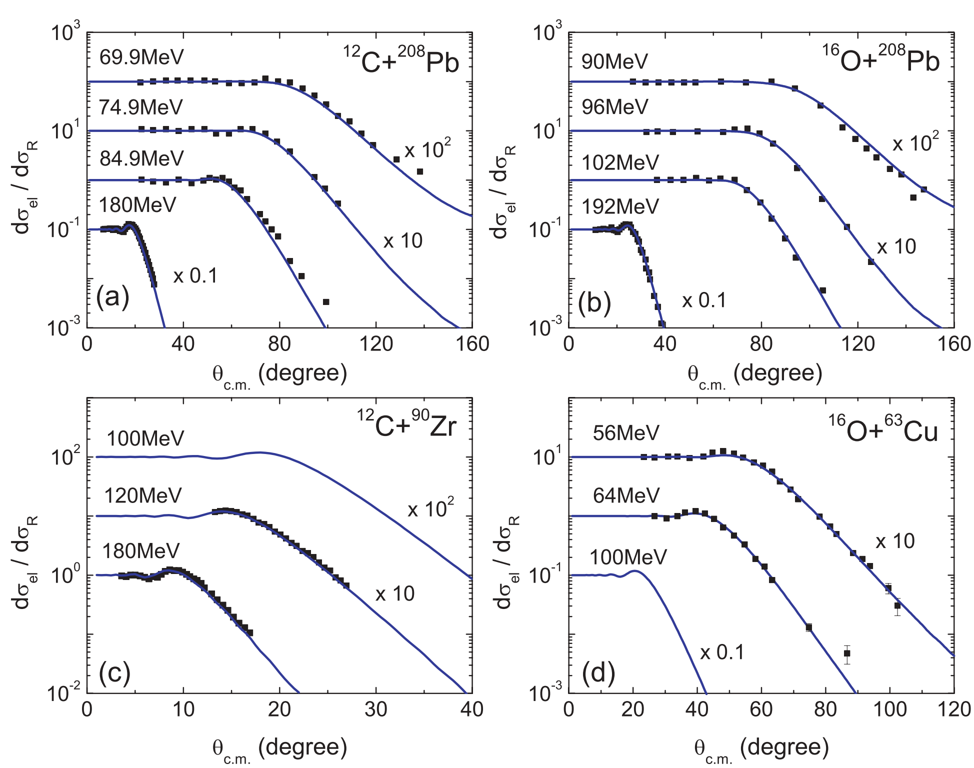

FIG. 1. (Color online) Elastic scattering angular distributions for the reactions $^{12}C + ^{208}Pb$, $^{16}O + ^{208}Pb$, $^{12}C + ^{90}Zr$, and $^{16}O + ^{63}Cu$ at different laboratory energies. The solid curves and the squares denote the calculated results with the modified Woods-Saxon potential and the experimental data, respectively. The experimental data are taken from Refs. [22–26].

potential depends on the incident energy at energies close to the Coulomb barrier and, when the center-of-mass energy is much higher than the Coulomb barrier energy, potentials deduced with the microscopic theory identify with the frozen density approximation [20]. We test the modified Woods-Saxon potential for the description of heavy-ion elastic scattering at energies much higher than the Coulomb barrier, because the reaction time is relatively short and the frozen density approximation seems to be applicable at these energies. Based on the optical model, we solve the Schroedinger equation for a given nucleus-nucleus potential using the traditional Numerov method to obtain the partial-wave scattering matrix that is used to describe the elastic scattering data [21]. The real and imaginary parts of the optical potential adopted in the calculations are described by the modified Woods-Saxon potential.

We have calculated the elastic scattering angular distributions for the reactions $^{12}C + {}^{208}Pb$, $^{16}O + {}^{208}Pb$, $^{12}C + {}^{90}Zr$, and $^{16}O + {}^{63}Cu$ at different laboratory energies. The calculated results (solid curves) are shown in Fig. 1, and the corresponding experimental data (squares) [22–26] are also presented for comparison. The experimental data of the four reactions at different energies are reasonably well reproduced by the modified Woods-Saxon potential in which the potential parameters are fixed.

We further test the MWS potential for the description of heavy-ion fusion at above barrier energies. At these energies, the fusion cross section is usually described by the classical formula

$$\sigma_{\text{fus}}(E_{\text{c.m.}}) = \pi R_f^2(1 - B/E_{\text{c.m.}}), \tag{5}$$

with the fusion radius R_f and the height of the fusion barrier B. Figure 2 shows the fusion excitation function of $^{16}O + {}^{208}Pb$. Taking B to be the barrier height B_0 (78.72 MeV) of the modified Woods-Saxon potential, the fusion cross sections at above barrier energies cannot be reproduced by the Eq. (5) (see the dash-dotted curve in Fig. 2). To describe the fusion cross sections satisfactorily, we introduced an empirical barrier distribution to take into account the multidimensional character of a realistic barrier due to the coupling to internal degrees of freedom of the binary system in our previous paper [9]. We proposed an effective weight function for describing the barrier distribution,

$$D_{\text{eff}}(B) = \begin{cases} D_1(B) & : \quad B < B_x \\ D_{\text{avr}}(B) & : \quad B \geqslant B_x \end{cases}, \tag{6}$$

where $D_{\text{avr}}(B) = (D_1(B) + D_2(B))/2$ and B_x is the left cross point of $D_1(B)$ and $D_2(B)$. $D_1(B)$ and $D_2(B)$ are two Gaussian functions [9,18] that depend on the barrier height B_0 of the modified Woods-Saxon potential. The effective weight function D_{eff} of the reaction ^{16}O+^{208}Pb is shown in the sub-figure of Fig. 2. Taking B to be the most probable barrier height $B_{\text{m.p.}}$ (74.43 MeV) according to the D_{eff}, the fusion cross sections at above barrier energies are reproduced reasonably well (see the solid curve in Fig. 2). With the empirical barrier distribution, the fusion cross sections and the mean barrier heights of a large number of reactions can be reproduced well [9,18,28].

From the above discussion, one finds that for the heavy-ion elastic scattering at above barrier energies the modified Woods-Saxon potential that is based on the frozen density approximation gives nice results. But the fusion cross section of the same reaction system can not be described well with the potential and the barrier distribution needs to be introduced to reproduce the fusion data. In a recently published article [29], the authors proposed two optical potentials for describing the reactions $^{12}C + {}^{208}Pb$ and $^{16}O + {}^{208}Pb$, respectively. Both the elastic scattering and fusion data can be satisfactorily described with the potentials at energies around the Coulomb barrier. At energies much higher than the Coulomb barrier (for example, $E_{\text{lab}} = 192$ MeV for $^{16}O + {}^{208}Pb$), the elastic scattering data cannot be reproduced well by the potential. In this work, we aim to find a nucleus-nucleus potential for describing the reactions systematically.

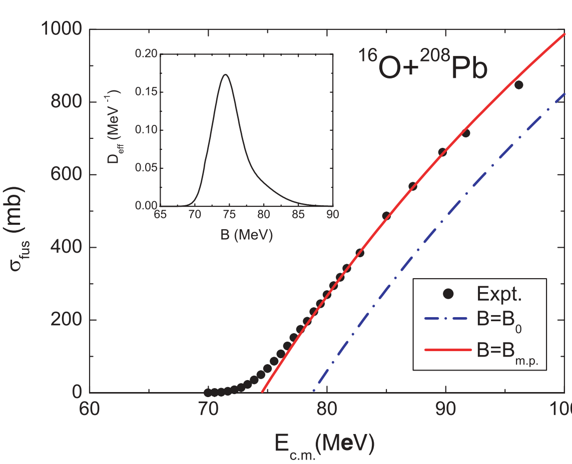

FIG. 2. (Color online) Fusion excitation function of the reaction $^{16}O + {}^{208}Pb$. The dash-dotted and solid curves denote the calculated results with Eq. (5) by taking $B = B_0$ and $B = B_{\text{m.p.}}$, respectively. The solid circles denote the experimental data [27]. The inset shows the effective weight function of the reaction.

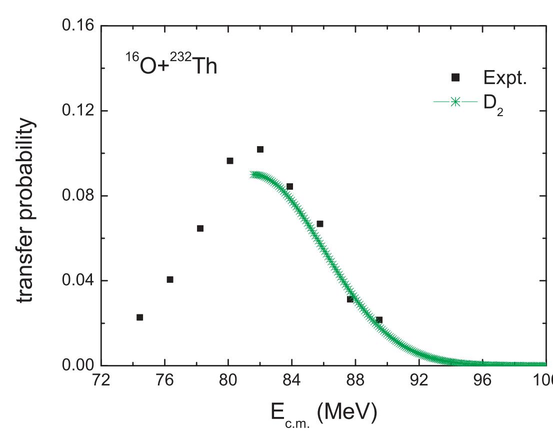

FIG. 3. (Color online) Transfer probability of $^{16}O + {}^{232}Th$. The squares denote the measured transfer probabilities [16] including the channels of 1p, 1p1n, 1α, 2p, and 2p1n transfers to the target nuclei. The crossed curve denotes the Gaussian function D_2 in the empirical barrier distribution.

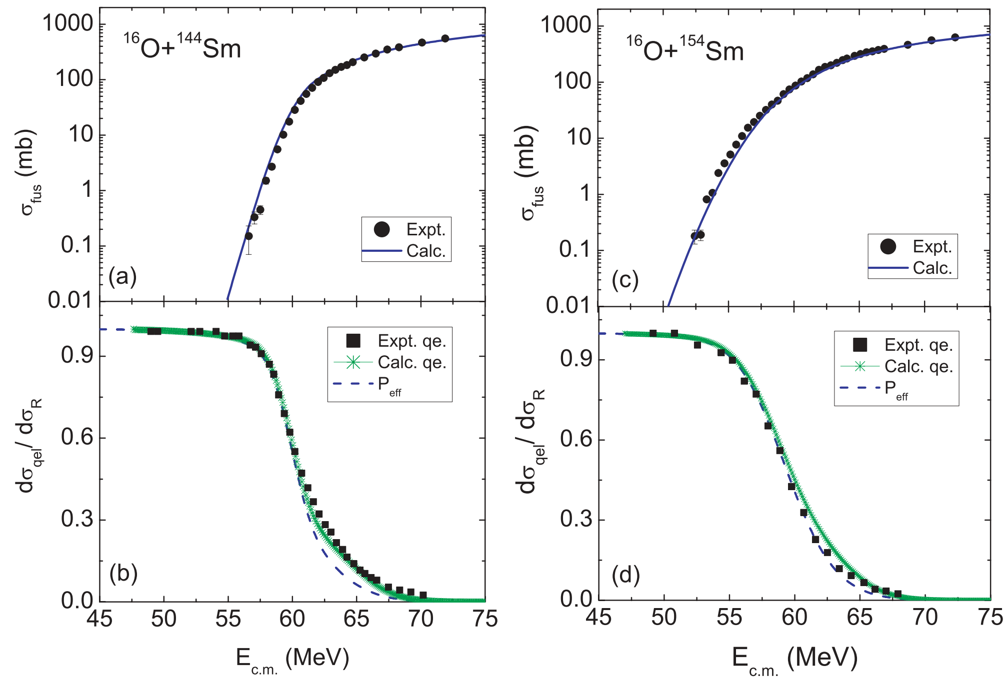

FIG. 4. (Color online) Fusion cross sections and quasi-elastic scattering cross sections as a function of energy for the reactions $^{16}O + ^{144}Sm$ and $^{16}O + ^{154}Sm$. The solid circles and squares denote the measured fusion cross sections σ_{fus} and quasi-elastic scattering cross sections, respectively. The solid curves in (a) and (c) denote the calculated results for σ_{fus}. The crossed curves in (b) and (d) denote the calculated results with Eq. (7). The dashed curves denote the results for P_{eff}. The experimental data of fusion and quasi-elastic scattering are taken from Refs. [4] and [5], respectively.

B. Description of large-angle quasi-elastic scattering

As a good counterpart of the fusion reaction, the large-angle quasi-elastic scattering is studied to explore the nucleus-nucleus potential. In this work, we explore the influence of the empirical barrier distribution proposed for the fusion reactions on the large-angle quasi-elastic scattering.

It is thought that the quasi-elastic differential cross section can be expressed as a weighted sum of the eigenchannel elastic differential cross sections under the adiabatic and iso-centrifugal approximation [30,31]. Similar to the description of fusion with the empirical barrier distribution, we describe the large-angle quasi-elastic scattering cross section with

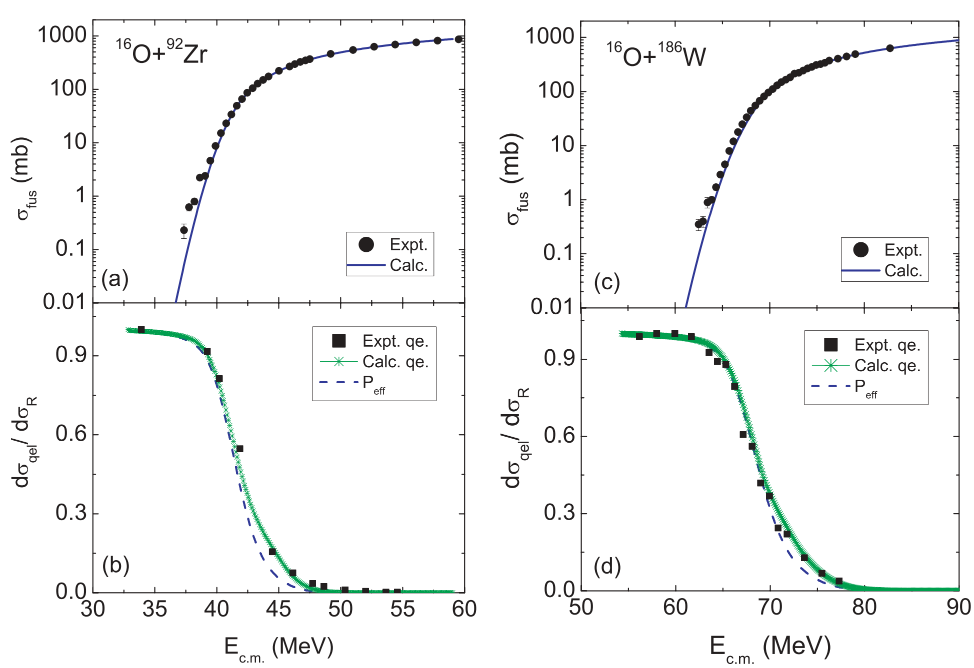

FIG. 5. (Color online) The same as Fig. 4, but for the reactions $^{16}O + ^{92}Zr$ and $^{16}O + ^{186}W$. The experimental data are taken from Refs. [4,5,34].

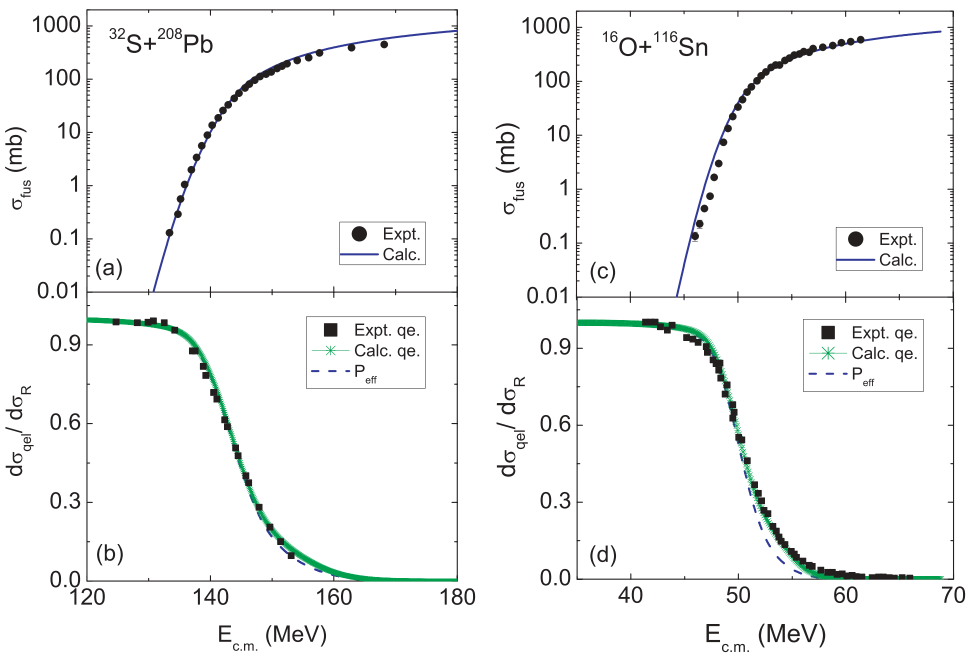

FIG. 6. (Color online) The same as Fig. 4, but for the reactions $^{32}S + {}^{208}Pb$ and $^{16}O + {}^{116}Sn$. The experimental data are taken from Refs. [35–37].

the effective weight function $D_{\rm eff}(B)$ at energies around the Coulomb barrier,

$$\frac{d\sigma_{\rm qel}}{d\sigma_R}(E_{\rm c.m.}) = P_{\rm eff} + P_{\rm corr}, \tag{7}$$

with

$$P_{\rm eff} = \frac{1}{F_0}\int_0^\infty D_{\rm eff}(B)\frac{d\sigma_{\rm el}}{d\sigma_R}(E_{\rm c.m.}, B)dB, \tag{8}$$

and $P_{\rm corr}$ is a small correction term. $\frac{d\sigma_{\rm el}}{d\sigma_R}$ is the ratio of the elastic cross section $\sigma_{\rm el}$ to the Rutherford cross section σ_R. F_0 is a normalization constant $F_0 = \int D_{\rm eff}(B)dB$. Within the semiclassical perturbation theory, a semiclassical formula for the backward scattering ($\theta = \pi$) is given [2,32],

$$\frac{d\sigma_{\rm el}}{d\sigma_R}(E_{\rm c.m.}, B) = \left(1 + \frac{V_N(R_c)}{E_{\rm c.m.}}\sqrt{\frac{Z_1Z_2e^2}{E_{\rm c.m.}}\frac{\pi}{a}}\right) \times \frac{\exp\left[-\frac{2\pi}{\hbar\omega}(E_{\rm c.m.} - B)\right]}{1 + \exp\left[-\frac{2\pi}{\hbar\omega}(E_{\rm c.m.} - B)\right]}. \tag{9}$$

Where the nuclear potential $V_N(R_c)$ is evaluated at the Coulomb turning point,

$$V_N(R_c) = \left(B - \frac{Z_1Z_2e^2}{R_f}\right)\left(\frac{1 + \exp[(R_f - R_0)/a]}{1 + \exp[(R_c - R_0)/a]}\right), \tag{10}$$

with the distance of the closest approach between two nuclei $R_c = Z_1Z_2e^2/E_{\rm c.m.}$. a is the diffuseness parameter of the nuclear potential. Z_1, Z_2, and $E_{\rm c.m.}$ denote the charge numbers of the projectile and target nuclei and the center-of-mass energy, respectively. R_f and $\hbar\omega$ are the barrier position and curvature of the modified Woods-Saxon potential, respectively.

The correction term $P_{\rm corr}$ in Eq. (7) takes into account some effects in the quasi-elastic scattering that are not involved in the empirical barrier distribution (which was proposed for describing fusion reactions). In this work, we assume that the correction term mainly comes from nucleon transfer. In principle, the transfer process also affects the fusion process and the effect of nucleon transfer may have been implicitly taken into account in the empirical barrier distribution. However the influence of nucleon transfer on the quasi-elastic scattering may differ from the influence on the fusion process, and a small correction term seems to be required.

For the quasi-elastic scattering, we first investigate the dependence of the transfer probabilities on the incident energies. The transfer probabilities $P_{\rm tr}$ can be written as $P_{\rm tr} = (d\sigma_{\rm tr}/d\Omega)/(d\sigma_{\rm R}/d\Omega)$, where $d\sigma_{\rm tr}/d\Omega$ is the transfer cross section [14]. At energies below the barrier the transfer probability increases with increasing incident energies because the distance of closest approach becomes small, leading to an increase in the nuclear overlap. At above barrier energies, on the contrary, the transfer probability decreases with increasing energies because the increased overlap results in more dissipative collisions that finally result in fusion [16]. For the transfer at energies below the barrier, we describe the transfer probability using the traditional semiclassical method that is mentioned previously in the Introduction. In this work, only the one-neutron transfer channels are taken into account for simplicity in the calculation of the transfer probability at subbarrier energies. For the transfer at energies above the barrier, we find the transfer probabilities are close to the Gaussian function D_2 of the empirical barrier distribution. For example, in Fig. 3 the measured transfer probabilities for the reaction $^{16}O + {}^{232}Th$ are compared with the corresponding Gaussian function D_2 of this reaction at energies above the barrier. The experimental data are in good agreement with D_2 at above barrier energies.

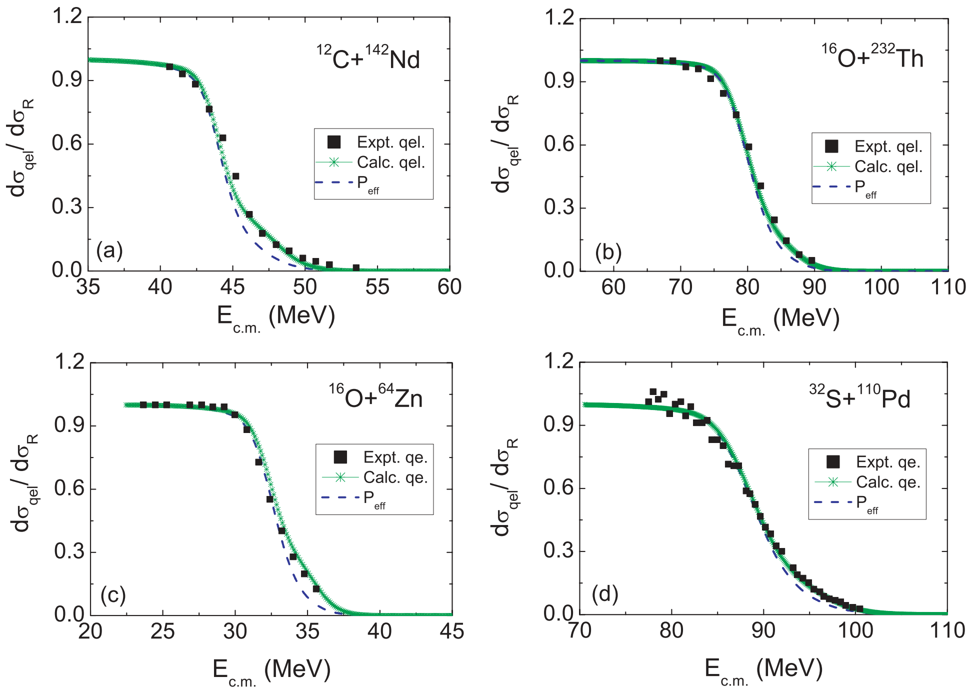

FIG. 7. (Color online) Quasi-elastic scattering cross sections as a function of energy for the reactions $^{12}C + {}^{142}Nd$, $^{16}O + {}^{232}Th$, $^{16}O + {}^{64}Zn$, and $^{32}S + {}^{110}Pd$. The squares and the crossed curves denote the measured and calculated quasi-elastic scattering cross sections, respectively. The dashed curves denote the calculated results for $P_{\rm eff}$.

Based on the above discussion, we write the transfer probability

$$P_{\rm tr}(E_{\rm c.m.}) = f \begin{cases} P_0 \exp(-2\alpha R_c) & : \quad E_{\rm c.m.} \leqslant B_m \\ D_2(E_{\rm c.m.}) & : \quad E_{\rm c.m.} \geqslant B_h \\ \left(1 + (F-1)\frac{B_h - E_{\rm c.m.}}{B_h - B_m}\right) D_2(E_{\rm c.m.}) & : \quad B_m < E_{\rm c.m.} < B_h \end{cases}, \tag{11}$$

with the strength factor $f = 1$ MeV. P_0 is a normalization constant given by $P_0 = D_2(B_0)/\exp(-2\alpha Z_1 Z_2 e^2/B_0)$ with the transfer form factor $\alpha = \sqrt{2\mu E_b/\hbar^2}$. μ is the reduced mass of the transferred nucleons, E_b is the effective binding energy of the transferred nucleons [33]. B_0 is the barrier height of the modified Woods-Saxon potential, B_m is the mean barrier height of the barrier distribution,

$$B_{\rm m} = \frac{\int B \; D_{\rm eff}(B)\, dB}{\int D_{\rm eff}(B)\, dB}. \tag{12}$$

We take $B_h = 2B_0 - B_m$ in this work. To have a smooth function for the transfer probability $P_{\rm tr}$ from subbarrier energies to above barrier energies, we introduce a function for $P_{\rm tr}$ in the energy region $B_m < E_{\rm c.m.} < B_h$ with a factor $F = \frac{P_0}{D_2(E_{\rm c.m.})}\exp(-2\alpha Z_1 Z_2 e^2/B_m)$ to link the two functions $P_0 \exp(-2\alpha R_c)$ and D_2 describing the $P_{\rm tr}$ at subbarrier and at above barrier energies, respectively.

We assume $P_{\rm corr} \approx P_{\rm tr}$. Both the fusion and quasi-elastic scattering cross sections of a series of reactions have been studied with the proposed approach in this work. Figures 4 to 6 show the calculated quasi-elastic scattering and fusion cross sections for the reactions $^{16}O + {}^{144}Sm$, $^{16}O + {}^{154}Sm$, $^{16}O + {}^{92}Zr$, $^{16}O + {}^{186}W$, $^{32}S + {}^{208}Pb$, and $^{16}O + {}^{116}Sn$. The experimental data [4,5,34–37] are also presented for comparison. The solid circles and squares denote the measured fusion cross sections $\sigma_{\rm fus}$ and large-angle quasi-elastic scattering cross sections, respectively. The solid curves in parts (a) and (c) of Figs. 4 to 6 denote the calculated results for $\sigma_{\rm fus}$ with the proposed empirical barrier distribution (see details in Refs. [9] and [18]). The crossed curves in parts (b) and (d) denote the calculated quasi-elastic scattering cross sections with Eq. (7). The dashed curves denote the results for $P_{\rm eff}$, i.e., the contribution of the empirical barrier distribution to the quasi-elastic scattering. We find that both the fusion excitation functions and the quasi-elastic scattering excitation functions of the six reactions can be satisfactorily well reproduced. In Fig. 7 we compare the measured quasi-elastic scattering excitation functions (squares) of the reactions $^{12}C + {}^{142}Nd$ [38], $^{16}O + {}^{232}Th$ [16], $^{16}O + {}^{64}Zn$ [39], and $^{32}S + {}^{110}Pd$ [40] with the calculated results with Eq. (7) (crossed curves). The calculated quasi-elastic scattering cross sections of the four reactions $^{12}C + {}^{142}Nd$, $^{16}O + {}^{232}Th$, $^{16}O + {}^{64}Zn$, and $^{32}S + {}^{110}Pd$ are in good agreement with the experimental data. Figures 4 to 7 indicate that the modified Woods-Saxon potential together with the empirical barrier distribution can simultaneously describe the quasi-elastic scattering and fusion of a number of reactions reasonably well.

III. CONCLUSION AND DISCUSSION

In this work, we have studied the heavy-ion elastic and large-angle quasi-elastic scattering with the same nucleus-nucleus potential proposed for describing fusion reactions. The elastic scattering angle distributions of a series of reactions at energies much higher than the Coulomb barrier can be reasonably well reproduced by the modified Woods-Saxon potential that is based on the frozen density approximation systematically. With the same potential the fusion cross sections at above barrier energies cannot be reproduced and an empirical barrier distribution (which takes into account the coupling of other degrees of freedom) is required to reproduce the fusion data. It seems that the coupling of other degrees of freedom to the relative motion of the nuclei is obvious in heavy-ion fusion processes whereas the frozen density approximation is applicable in the elastic scattering process at energies much higher than the Coulomb barrier. With the empirical barrier distribution function based on the modified Woods-Saxon potential, the fusion cross sections of a series of reactions have been well reproduced. Further, with the same empirical barrier distribution and taking into account the correction term that mainly comes from the nucleon transfer, the calculated large-angle quasi-elastic scattering cross sections of these reactions are in good agreement with the experimental data.

ACKNOWLEDGMENTS

One of the authors (N. Wang) is grateful to Prof. Yongxu Yang for providing a code to calculate elastic scattering angular distribution and for fruitful discussions. This work is supported by the National Natural Science Foundation of China, No. 10465001.

[1] Z. F. Muhammad, K. Hagino, S. Mitsuoka, and H. Ikezoe, Phys. Rev. C **77**, 034604 (2008).
[2] K. Hagino and N. Rowley, Phys. Rev. C **69**, 054610 (2004).
[3] N. Rowley, G. R. Satchler, and P. H. Stelson, Phys. Lett. **B254**, 25 (1991).
[4] J. R. Leigh *et al.*, Phys. Rev. C **52**, 3151 (1995).
[5] H. Timmers *et al.*, Nucl. Phys. **A584**, 190 (1995).
[6] R. K. Gupta, M. Manhas, G. Munzenberg, and W. Greiner, Phys. Rev. C **72**, 014607 (2005).
[7] V. I. Zagrebaev, Phys. Rev. C **64**, 034606 (2001).
[8] G. G. Adamian *et al.*, Nucl. Phys. **A633**, 409 (1998).
[9] M. Liu, N. Wang, Z. Li, X. Wu, and E. Zhao, Nucl. Phys. **A768**, 80 (2006).
[10] H. Timmers *et al.*, J. Phys. G: Nucl. Part. Phys. **23**, 1175 (1997).
[11] A. Mukherjee, D. J. Hinde, M. Dasgupta, K. Hagino, J. O. Newton, and R. D. Butt, Phys. Rev. C **75**, 044608 (2007).
[12] Z. F. Muhammad and K. Hagino, Phys. Rev. C **77**, 014606 (2008).
[13] R. Bass, *Nuclear Reactions with Heavy Ions* (Springer, Berlin, 1980).
[14] K. E. Rehm, Annu. Rev. Nucl. Part. Sci. **41**, 429 (1991).
[15] J. F. Liang, L. L. Lee Jr., J. C. Mahon, and R. J. Vojtech, Phys. Rev. C **47**, R1342 (1993).
[16] S. Sinha, R. Varma, R. K. Choudhury, B. K. Nayak, A. Saxena, R. G. Thomas, and B. V. Dinesh, Phys. Rev. C **61**, 034612 (2000).
[17] B. J. Roy *et al.*, Nucl. Phys. **A588**, 706 (1995).
[18] N. Wang, K. Zhao, W. Scheid, and X. Wu, Phys. Rev. C **77**, 014603 (2008).
[19] A. Dobrowolski, K. Pomorski, and J. Bartel, Nucl. Phys. **A729**, 713 (2003).
[20] K. Washiyama and D. Lacroix, arXiv:0804.2823 (2008).
[21] Y.-X. Yang and Q.-R. Li, Phys. Rev. C **72**, 054603 (2005).
[22] S. Santra, P. Singh, S. Kailas, A. Chatterjee, A. Shrivastava, and K. Mahata, Phys. Rev. C **64**, 024602 (2001).
[23] C.-C. Sahm *et al.*, Phys. Rev. C **34**, 2165 (1986).
[24] F. Videbaek *et al.*, Phys. Rev. C **15**, 954 (1977).
[25] J. B. Ball *et al.*, Nucl. Phys. **A252**, 208 (1975).
[26] R. Lichtenthäler, D. Pereira, L. C. Chamon, L. C. Gomes, A. Ventura, and L. Zuffi, Phys. Rev. C **50**, 3033 (1994).
[27] C. R. Morton, A. C. Berriman, M. Dasgupta, D. J. Hinde, J. O. Newton, K. Hagino, and I. J. Thompson, Phys. Rev. C **60**, 044608 (1999).
[28] N. Wang, Z. Li, and W. Scheid, J. Phys. G: Nucl. Part. Phys. **34**, 1935 (2007).
[29] B. Sahu, G. S. Mallick, B. Sahu, S. K. Agarwalla, and C. S. Shastry, Phys. Rev. C **77**, 024604 (2008).
[30] M. V. Andres, N. Rowley, and M. A. Nagarajan, Phys. Lett. **B202**, 292 (1988).
[31] H. Zhang *et al.*, Phys. Rev. C **57**, R1047 (1998).
[32] S. Landowne and H. H. Wolter, Nucl. Phys. **A351**, 171 (1981).
[33] Angela Bonaccorso, Acta Phys. Pol. B **30**, 1421 (1999).
[34] J. O. Newton, C. R. Morton, M. Dasgupta, J. R. Leigh, J. C. Mein, D. J. Hinde, H. Timmers, and K. Hagino, Phys. Rev. C **64**, 64608 (2001).
[35] H. Timmers *et al.*, Nucl. Phys. **A633**, 421 (1998); and the doctoral thesis of H. Timmers.
[36] E. Piasecki *et al.*, Phys. Rev. C **65**, 054611 (2002).
[37] Vandana Tripathi, Lagy T. Baby *et al.*, Phys. Rev. C **65**, 014614 (2001).
[38] H. Majumdar, C. Basu, P. Basu, S. Roy, K. Mahata, S. Santra, A. Chatterjee, and S. Kailas, Phys. Rev. C **68**, 017602 (2003).
[39] J. F. P. Huiza, E. Crema, D. S. Monteiro, J. M. B. Shorto, R. F. Simoes, N. Added, and P. R. S. Gomes, Phys. Rev. C **75**, 064601 (2007).
[40] O. A. Capurro, J. E. Testoni, D. Abriola, D. E. DiGregorio, G. V. Marti, A. J. Pacheco, and M. R. Spinella, Phys. Rev. C **61**, 037603 (2000).